32nd URSI GASS, Montreal, 19-26 August 2017

Combined TID observation by ionosonde and dense GPS/GLONASS network

Ruslan O. Sherstyukov*, Adel D. Akchurin, Oleg N. Sherstyukov
Kazan Federal University, 18 Kremlyovskaya street, 420008, http://kpfu.ru

Abstract

Simultaneous observations of the ionosphere using the ionosonde and dense GPS / GLONASS receivers network allow us to investigate TIDs parameters by two independent methods. Two-dimensional TEC perturbation maps using 150 GPS / GLONASS receivers were obtained. The distance between the network cells is about 40 km and the temporal resolution of the network is 30 seconds. The ionosonde works in one minute cadence. The ionosonde located inside the GPS / GLONASS sounding area. Daytime MSTIDs with wavefronts stretching in NE–SW direction are observed on TEC maps. These structures propagate southeastward at the velocity of 100– 150 m/s. Their wavelengths are 250-300 km and amplitudes are larger than 0.4 TECU. For the same time the ionogram variations of F_2-peak plasma frequency with peak-to-peak amplitude near 0.3 MHz are observed. The periods of TEC perturbations and F_2-peak frequency variations are close (~40 min). The maximum deviation of F_2-peak frequency corresponds to minimum value of TEC perturbation over the ionosonde.

1. Introduction

Perturbations of TEC known as traveling ionospheric disturbances (TIDs), which have been studied with several observational techniques, such as ionosondes [Bowman et al., 1990], incoherent scatter (IS) radars [Oliver et al., 1997], satellite beacons [Jacobson et al., 1995], and HF Doppler radars [Waldock and Jones, 1986], GNSS methods [Saito et al., 1998]. For various reasons, separately these methods cannot provide continuous temporal and spatial map of TIDs location with wide horizontal and vertical coverage.

The appearance of the dense network of GPS receivers gave impetus to the observations of ionospheric irregularities with new two-dimensional and three-dimensional ionosphere reconstruction techniques [Tsugawa et al., 2007, Seemala et al., 2014]. The spatial horizontal dimension of irregularities, which is able to observe by a network of GPS receivers depend on the distance between the network cells. The GPS methods characterized by strong azimuthal dependence of TEC response for some ranges of TIDs directions. Consequently, some TIDs can become lower than the noise of phase measurements [Afraimovich et al.,2000]. The ionosonde observations seem can detect all TIDs passing over head with $\Delta N/N > 10\%$. The threshold value of $\Delta N/N>10\%$ derived due to the absence of reliable investigations, which shows that ionosondes can observe irregularities with a scale size less than those that LSTIDs have. These irregularities can travel to equatorial direction on 1000 km distance without much attenuation and with velocity of 400-700 m/s [Evans et al., 1983]. The LSTIDs $\Delta N/N$ values are considered more than 10%. All multi-instrumental observations with ionosonde assistance were focused on LSTIDs estimation during the geomagnetic storm periods [Habarulema et al., 2013, Ding et al., 2013]. For the LSTIDs estimation the *foF2*, and *hmF2* ionosonde parameters are only used. However, the ionograms can contain different signatures such as spread F (double trace), V-shaped traces [see Bowman, 1991], U-shaped traces [see Lobb, 1977], hooks [see Cooper, Cummack, 1986] traditionally attributed to MSTIDs. The compared ionosonde and dense GPS/GLONASS network data will allow us to verify the knowledge about TIDs parameters obtained by different methods, to find ionogram signatures appropriated to MSTIDs.

2. Method and Results

In this study we use the data from a dense GPS / GLONASS receiver's network and the data from the ionosonde working in the minute cadence. More than 150 GPS / GLONASS receiving points were used. Figure 1

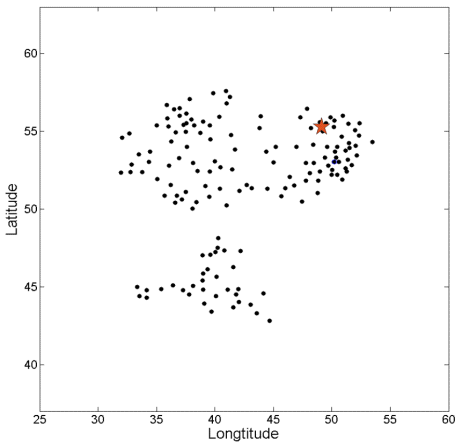

Figure 1. Location of GPS/GLONASS and ionosonde. Dots represent the locations of the GPS/GLONASS receivers. Red start represent the location of the ionosonde.

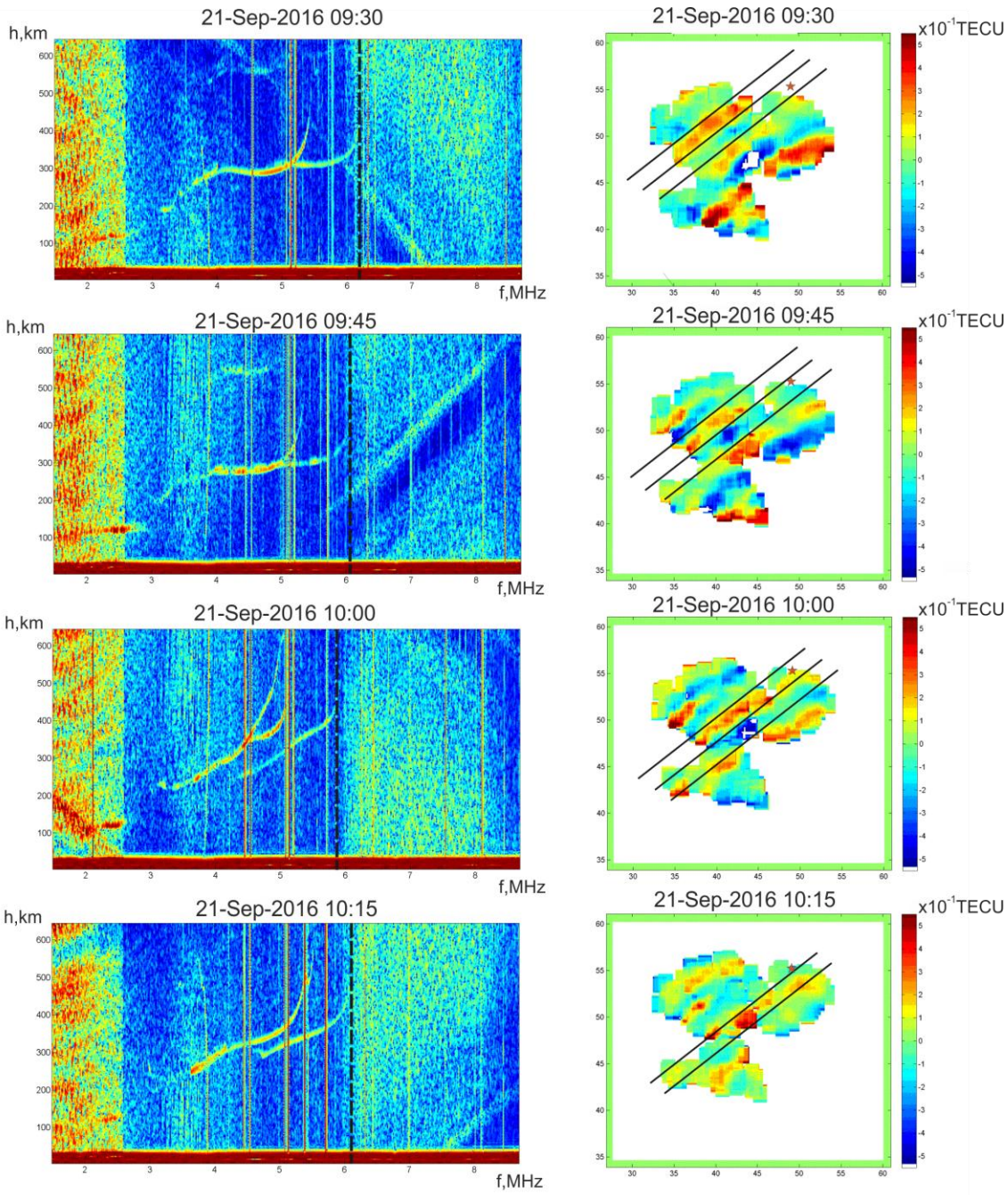

Figure 2. Two-dimensional TEC perturbation maps on the right sight of figure and ionograms on the left side of figure. Dashed black line in the ionograms shows F_2 peak frequency. Red star in TEC maps represent the ground location of the ionosonde, solid lines represent the wavefronts of band structures.

shows the location of the ionosonde and GPS/GLONASS receivers.

All GPS/GLONASS receivers provide the data of carrier phase and pseudo-range measurements in two frequencies (f_1 = 1575.42 MHz, f_2 = 1227.60 MHz for GPS receivers and f_1=1602+n×0,5625 MHz , f_2= 1246 MHz +n×0.4375 MHz for GLONASS receivers, there n is the number of frequency channel (n =−7,−6,−5,…0,…,6,). The data of GPS/GLONASS data are converted to two-dimensional TEC perturbation maps for TID investigation.

The TEC value for each pixel of two dimensional TEC map is an average of perturbations for all line-of-sight (LOS) between receiver and satellite, which crossed the pixel at 300 km altitude (the approximate F-region peak height). The size of each pixel is 0.15×0.15 in latitude and longitude. TEC map in each epoch is smoothed spatially

with the running average of 5×5 pixel (0.75×0.75) in latitude and longitude.

Figure 2 shows the ionograms and the two-dimensional maps of detrended TEC over European part of Russia in the daytime between 13:30 LT (09:30 UT) and 14:15 LT (10:15 UT) on September 21, 2016 with a 15-minute interval. The data from both GPS (G18) and GLONASS (R03) satellites were used. Band-like structures with wavefronts stretching in NE –SW direction are seen in the TEC maps. From their wave parameters the band structures can be identified as the daytime MSTIDs observed in Southern California [Kotake et al., 2007]. These structures propagate southeastward at the velocity of 100–150 m/s. Their wavelengths are 250-300 km and amplitudes are larger than 0.4 TECU. For the same time the F_2-peak plasma frequency variations in the ionograms with peak-to-peak amplitude near 0.3 MHz are observed. The periods of TEC perturbations and F_2-peak frequency variations are close (~40 min). The maximum deviation of F_2-peak frequency corresponds to minimum value of TEC perturbation over the ionosonde.

The hooks signatures (V-shaped traces) with 8-12 minutes lifetime in the ionograms are also observed (see figure 3). These signatures traditionally attributed to MSTIDs in ionosonde observations. But in our investigation their periods doesn't match with TEC perturbations period as a response on daytime MSTIDs by dense GPS/GLONASS network.

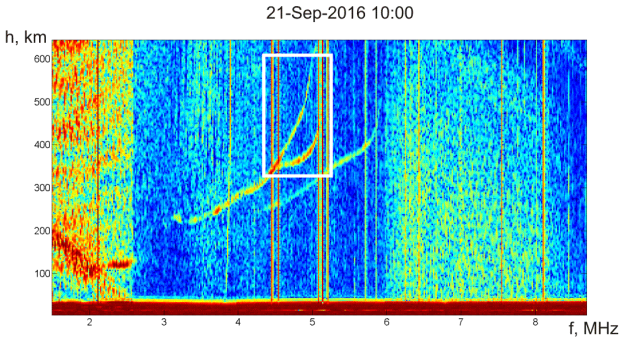

Figure 3. Ionogram with hook signature. The hook signature is circled by the white quadrate.

3. Conclusions

The existed point of view that ionosondes can estimate only LSTIDs (plasma perturbations with scale size ΔN/N >10%) was dominated. It was based on the one of the striking LSTIDs feature, that they can travel a distance of 1000 km without much attenuation. These features allow LSTID observation equipment with low sensitivity to plasma perturbations to be placed at 500 km distance [Evans et al., 1983]. So the value ΔN/N of such perturbations is clearly more than 10%. Presently, only such ionosonde measurements are generally performed.

In our study we show that estimation of MSTIDs by ionosonde methods is a possible task. We use TEC maps to find plasma perturbations with daytime MSTIDs parameters. For a daytime MSTIDs with velocity of 100–150 m/s, 250-300 km wavelengths, 40 minutes TEC periods and amplitudes larger than 0.4 TECU, the variations of F_2 peak frequency with 40 minutes period were found. At the same time the hook signatures were observed. But the lifetime of these hook signatures doesn't match with MSTIDs period, so the scale size of perturbations associated with hooks is less than those of MSTIDs, at least in these investigations.

4. Acknowledgements

The work is performed according to the Russian Government Program of Competitive Growth of Kazan Federal University.

5. References

1. E.L. Afraimovich., K.S. Palamartchouk. N.P. Perevalova, Statistical Angle-of-arrival and Doppler Method for GPS radio interferometry of TIDs, *Advances in Space Research*, **26**, 6, 2000, pp. 1001-1004

2. G. G. Bowman, A review of some recent work on mid-latitude spread-F occurrence as detected by ionosondes, *Journal of Geomagnetism and Geoelectricity*, **42**, 1990, pp. 109-138

3. J. Cooper, C.H. Cummack, The analysis of a travelling ionospheric disturbance with non-linear ionization response, *Journal of Atmospheric and Terrestrial Physics*, **48**, 1, 1986, pp. 61-71

4. F. Ding, W. Wan, B. Ning, B. Zhao, Q. Li, Y. Wang, L. Hu, R. Zhang, B. Xiong, Observations of poleward-propagating large-scale traveling ionospheric disturbances in southern China, *Annales Geophysicae.*, **31**, 2013, pp. 377–385

5. J. V. Evans, J. M. Holt, R. H. Wand, A differential-Doppler study of traveling ionospheric disturbances from Millstone Hill, *Radio Science*, **18**, 3, 1983, pp. 435-451

6. A. Fukao, Climatology of F region gravity wave propagation over the middle and upper atmosphere radar, *Journal of Geophysical Research*, **102**, 1997, pp. 14,499-14,512

7. J. B. Habarulema, Z. T. Katamzi, L.-A. McKinnell, Estimating the propagation characteristics of largescale traveling ionospheric disturbances using ground-based and satellite data, *Journal of Geophysical Research: Space Physics*, **118**, 2013, pp. 7768–7782

8. A.R. Jacobson, R.C. Carlos, R.S. Masseya , G. Wu, Observations of traveling ionospheric disturbances with a satellite beacon radio interferometer: Seasonal and local time behavior, *Journal of Geophysical Research*, **100**, 1995, pp. 1653-1665

9. N. Kotake, Y. Otsuka, T. Ogawa, T. Tsugawa, A. Saito, Statistical study of medium-scale traveling ionospheric disturbances observed with the GPS networks in Southern California, *Earth Planets Space*, **59**, 2007, pp. 95– 102

10. R.J. Lobb, Titheridge J.E., The effects of travelling ionospheric disturbances on ionograms, *Journal of Geophysical Research*, **39**, 1977, pp. 129-138

11. W.L. Oliver, Y. Otsuka, M. Sato, T. Takami, S. Saito A. and S. Fukao, High resolution mapping of TEC perturbations with the GSI GPS network over Japan, *Geophysical Research Letters*, **25**, 16, 1998, pp. 3079-3082

12. Gopi K. Seemala, Mamoru Yamamoto, Akinori Saito, Chia-Hung, Three-dimensional GPS ionospheric tomography over Japan using constrained least squares, *Journal of Geophysical Research: Space Physics*, **119**, 2014, pp. 3044–3052, doi:10.1002/2013JA019582

13. T. Tsugawa, Y. Otsuka, A. J. Coster, A. Saito, Medium-scale traveling ionospheric disturbances detected with dense and wide TEC maps over North America, *Geophysical Research Letters*, **34**, 2007, doi:10.1029/2007GL031663

14. J. A. Waldock, T. B. Jones, HF Doppler observations of medium-scale travelling ionospheric disturbances at midlatitudes, *Journal of Atmospheric and Terrestrial Physics*, **8**, 1986, pp. 245-260